Chapter 4

Structural and mathematical analyses of a dual-sided metasurface structure for the design of multifunctional and bidirectional optoelectronics devices

4.1. Introduction

Multifunctionality of electronic devices has been a long-lasting pursuit for the electronic system, especially if the functions are mutually exclusive from one another. Most of the metasurface devices are based on single-sided metasurface structure employing a periodic metallic pattern-dielectric-metal configuration, where the dielectric layer is sandwiched between the top layer comprising metallic pattern and bottom metallic plate. Such single-sided metasurface structures are mostly used as an absorber in stealth technology for reducing the radar cross section area [74-75]. However, the presence of metallic plate at the bottom completely blocks the entire frequency band. This causes a fatal problem in the wireless communication system, where apart from absorbing a certain band of frequency, another band of frequency needs to be transmitted to communicate with other remote devices. A multifunctional device that offers absorption and transmission in two separate bands of frequencies is referred as “rasorber” [76-77]. Most of them have used passive circuit elements such as resistance, inductance, capacitance for their realization [78-79]. Due to the presence of vias for the realization of inductance, such devices are difficult to realize in practice. Later, re-configurable rasorber based on PIN diode has been reported in [80], which switches the mode of operation from absorption to transmission by applying suitable bias voltage across the diode. However, the presence of PIN diode in the bottom makes only one layer re-configurable. In

[81], both the layers are made re-configurable by embedding the top layer with PIN diode and bottom layer with varactor diode. However, there are two main challenges associated with such designs. Firstly, they are not realizable at high frequencies such as THz, infrared etc. Moreover, such designs limit the directional efficiency of the device, as they can be used for single side incidence only, since the bottom layer is completely grounded.

Recently, very few rasorbers have been reported which has not used any passive or active elements in its design. In [82], a rasorber in microwave frequency region has been reported which consists of three metallic layers separated by three different dielectrics in between. The structure offers a low transmission value of 41%. In [83], a rasorber has been proposed, which exhibits a maximum transmission value of 63.8%. The main issue with these designs is their low transmissivity and directional sensitivity (unidirectional). Additionally, the evolution of the geometry has not been discussed. Without understanding the role of different metasurface layers on the frequency response, it is extremely tedious to realize a single structure offering multifunctionality by merely optimizing the shapes and dimensions of the metallic pattern.

In this regard, an elaborative study on the structural and mathematical analyses of a dual-sided metasurface structure has been carried out in this chapter. The work elucidates that the ratio between the resonating wavelength and the structure's thickness plays a deterministic role in switching the mode of application from absorption to transmission or vice versa. Further, to add directional insensitivity (bidirectionality) to a rasorber, the equivalent circuit model (ECM) of the dual-sided metasurface structure has been explored. The mathematical findings suggest that the impedance of the two metasurface layers plays a crucial role in designing the bidirectional rasorber. The studied have been later validated by designing a bidirectional rasorber. The study on dual-sided metasurface structures can pave the way to design multifunctional or bidirectional optoelectronic devices.

4.2. Study of a dual-sided metasurface structure

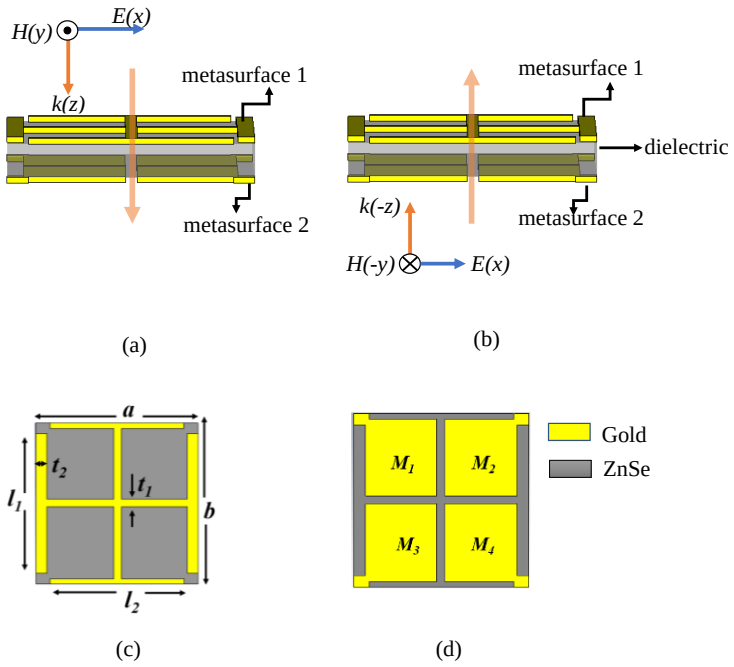

Fig. 4.1. 3-D perspective view of the unit-cell of the dual-sided metasurface for (a) +*z* incidence (b) -*z* incidence, along with the (c) metallic pattern at metasurface 1 and (d) metallic pattern at metasurface 2 ($a = b = 3.29\ \mu m$, $l_1 = 2.9\ \mu m$, $l_2 = 2.83\ \mu m$, $t_1 = 0.15\ \mu m$, $t_2 = 0.23\ \mu m$).

A dual-sided metasurface structure consisting of dielectric layer in between top and bottom layers is shown in Fig. 4.1. The perspective view of the structure along with the electromagnetic field vectors for +*z* incidence (metasurface 1 to metasurface 2) and -*z* incidence (metasurface 2 to metasurface 1) is shown in Fig. 4.1 (a) and Fig. 4.1 (b) respectively. The top view of the metallic patterns of metasurface 1 and metasurface 2 layers are shown in Fig. 4.1 (c) and Fig. 4.1 (d) respectively. The uniqueness in the design is the selection of complementary sets of metallic patterns at the top (Fig. 4.1 (c)) and bottom metasurface layers (Fig. 4.1 (d)). Here, the term "complementary" signifies that the non-metallic (open) region of metasurface 1 exactly finds a metallic pattern just beneath it at metasurface 2 (marked as M_1, M_2, M_3, M_4). The role of the complementary sets of metallic patterns is to minimize the transmission from the structure. The electromagnetic [EM] waves that enter through the open region of metasurface

1(2), finds a metallic region just under it at metasurface 2(1) and thus cannot get transmitted out. However, it is not compulsory that the two metasurface patterns should always be complementary. Based on the applications, the selection of metallic pattern could be of any random shape or size.

All the simulations have been done in CST Microwave Studio based on Finite Integration Technique (FIT), considering the periodic boundary conditions. For the metallic components, gold has been taken due to its low ohmic loss, better chemical stability, and ease in fabrication at high frequencies. The dielectric constant of gold is modelled using Drude model, which provides a realistic characterization of metals at high frequencies. The thickness of the dielectric layer is optimized as 0.41 μm, while that of gold has been taken as 0.055 μm. For dielectric, ZnSe has been taken due to its good thermal and mechanical properties at infrared frequencies. The dielectric permittivity of ZnSe has been taken from the experimental results given in.

4.2.1 Frequency response for change in the direction of incidence

The study suggests that any dual-sided metasurface structure always exhibits two resonance frequencies, where one of the frequencies lies on the low-frequency side while the other one lies on the high-frequency side. The reflection coefficient responses of the dual-sided metasurface structure are shown in Fig. 4.2. It is evident from the responses that the dual-sided metasurface whose unit cell is shown in Fig. 4.1 exhibits two resonance frequencies at 10.4 THz and 32.5 THz for $+z$ incidence and 10.4 THz and 47.5 THz for $-z$ incidence, as shown in Fig. 4.2(a) and Fig. 4.2(b) respectively. The reason for the low reflection coefficient value at the resonating frequencies can be explained by retrieving the effective impedance of the dual-sided metasurface structure from the reflection and transmission coefficient data for both $+z$ and $-z$ incidences, as shown in Fig. 4.3(a) and Fig. 4.3(b) respectively. It can be observed that at low (10.4 THz) and high (32.5 THz, 47.5 THz) resonance frequencies, the effective

impedance of the dual-sided metasurface structure is nearly equal to the intrinsic impedance of the air (1), signifying an impedance matching condition corresponding to the incident EM wave.

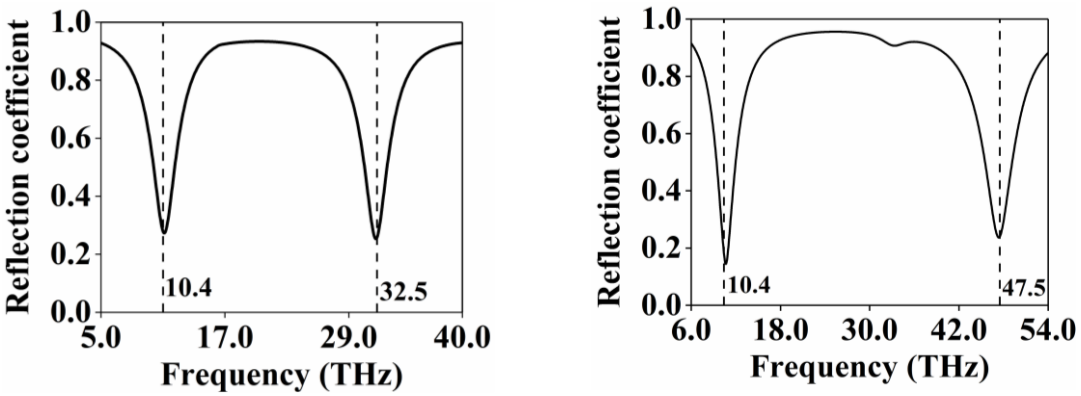

(a) (b)

Fig. 4.2. Reflection coefficient responses of the dual-sided metasurface design provided in Fig. 4.1 for (a) +*z* incidence and (b) -*z* incidence.

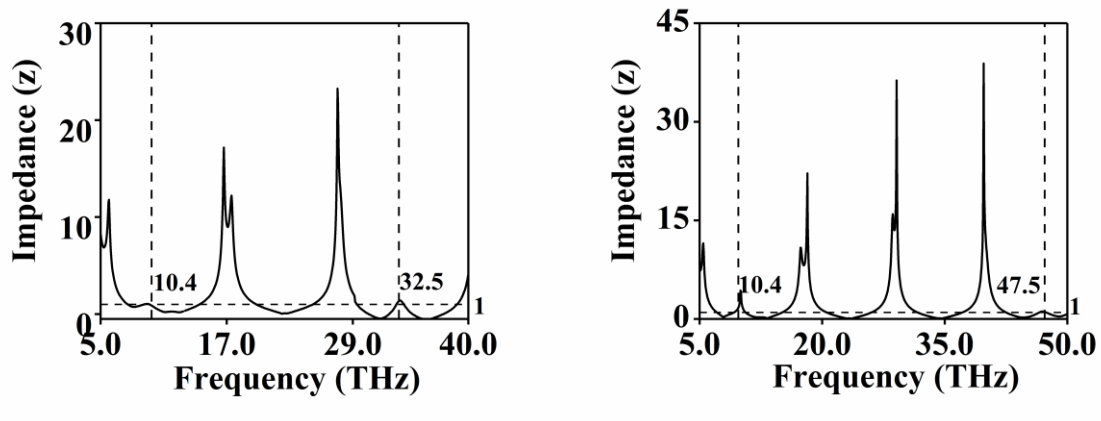

(a) (b)

Fig. 4.3. Variation of the effective impedance of the dual-sided metasurface structure at low and high resonance frequencies of (a) +*z* and (b) -*z* incidence.

Unlike the single-sided metasurface, a dual-sided metasurface structure consists of periodic sub-wavelength metallic patterns at the bottom; thereby making the explicit study of the transmission characteristics.

The transmission coefficient response of the dual-sided metasurface structure is shown in Fig. 4.4. It is evident that the structure offers a high transmission coefficient value of 0.8 in the low frequency region and thus works as a band pass filter. On the contrary, the structure works like an absorber in the high frequency region by exhibiting a low transmission coefficient value of 0.28 and 0.24 at 32.5 THz and 47. 5 THz respectively.

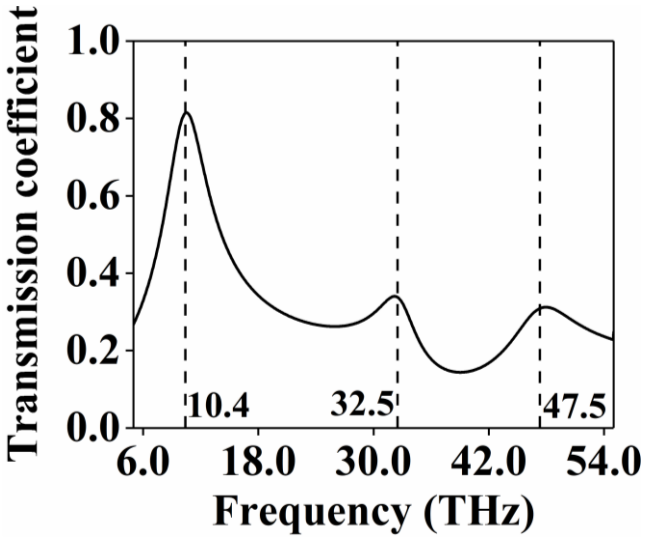

Fig. 4.4. Transmission coefficient response of the structure at 10.4 THz, 32.5 THz, and 47.5 THz.

4.3. Multifunctionality in the light of wave-structure interaction

The reason for the change in the mode of operation from transmission at low resonance frequency to absorption at high resonance frequency has been elaborated in the light of wave-structure interaction. The two main factors in the analysis of wave-structure interaction are the size of the structure and wavelength of the incident electromagnetic wave. When the wave interacts with the structure much smaller than the wavelength, then the change experienced by the wave is so small that the wave shows negligible interference with the intermediate layers and thus moves in a straight path. The effect gets recognizable when the ratio between the wavelength of the wave and size of the structure gradually becomes comparable to each other.

At low resonance i.e., 10.4 THz, when the resonating wavelength is large, the structure's thickness (h) is very small compared to the resonating wavelength ($h \approx \frac{\lambda}{70}$). For such a small thickness (compared to the resonating wavelength), the wave cannot distinguish different layers of the structure and therefore acknowledge the whole structure as a single entity having an effective impedance value [84]. The frequency for which the effective impedance of the structure matches with the intrinsic impedance of the air, the wave incident on metasurface 1(2) gets transmitted out from metasurface 2(1) without getting affected by the intermediate layers, as evident from a high transmission value.

In contrast, when the frequency of resonance increases i.e., when the resonating wavelength is small, the thickness of the structure becomes more comparable to the resonating wavelength. For example, at 32.5 THz and 47.5 THz, the ratio of the structure's thickness and resonating wavelength increases to $\frac{\lambda}{22}$ and $\frac{\lambda}{15}$ respectively. The incident EM wave can now distinguish three different layers of the structure and thereby acknowledge the presence of complementary set of metallic patterns at the top and bottom metallic layer, responsible for low transmission coefficient value.

Fig. 4.5 depicts the variation in the transmission coefficient response with increase in the frequency. The variation in the frequency has been done by decreasing the length l_1 of the metallic pattern of the top metasurface. It can be seen that the variation in the length l_1 only varies the high frequency point with negligible variation is seen in the low resonance frequency. Also, it can be seen that with each decrement in l_1, the high frequency point undergoes a blue shift with a steady reduction in the transmission coefficient value. The result validates that at low resonance frequency the interaction of incident EM wave with the metallic layers is not perceptible. Therefore, any change in the dimension of the metallic pattern is not evident in the transmission coefficient response at the low resonance frequency. On the contrary, at high

resonance frequency, the size of the structure becomes more comparable with the resonating wavelength, result in a subsequent decrease in the transmission coefficient value.

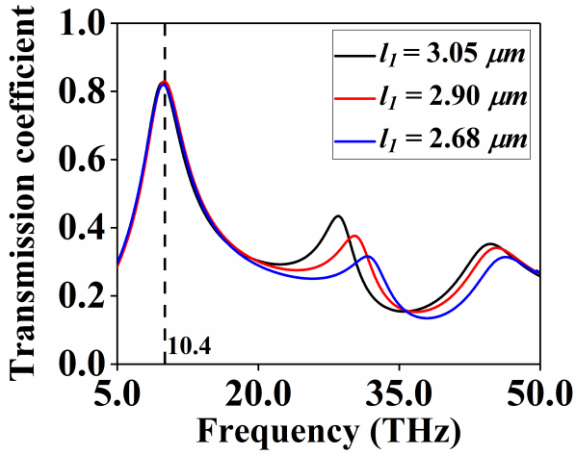

Fig. 4.5. Variation in the transmission coefficient response with increase in the frequency.

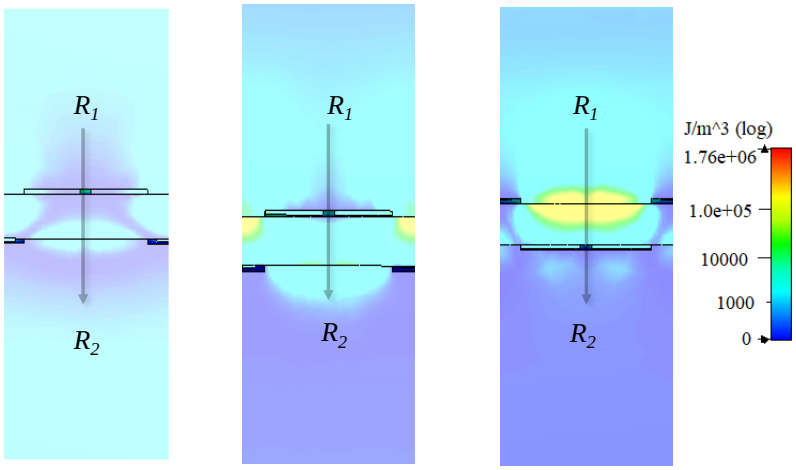

(a) 10.4 THz (b) 32.5 THz (c) 47.5 THz

Fig. 4.6. Electric energy density plot at the three resonance frequencies (a) 10.4 THz (b) 32.5 THz and (c) 47.5 THz.

Moreover, to reinforce the argument on wave-structure interaction, a descriptive study based on electric energy density plot of the dual-sided metasurface structure in the XZ cross section has been evaluated at the three resonance frequencies viz., 10.4 THz, 32.5 THz and 47.5 THz. Fig. 4.6 presents the electric energy density plot at the three resonance frequencies, where R_1 and R_2 are respectively the air boundaries above and below the metasurface structure. It can

be depicted from Fig. 4.6 (a), that at 10.4 THz, the electric energy density distribution in region R_1 is identical to that in region R_2, signifying a complete transmission at low frequency. On the contrast at high resonance frequencies viz., 32.5 THz (Fig. 4.6 (a)) and 47.5 THz (Fig. 4.6 (b).), the electric energy density in region R_2 is approximately zero, signifying a complete absorption.

4.4 Equivalent circuit models of dual-sided metasurface at low resonance frequencies

The frequency of resonance depends on the effective impedance of the structure. Therefore, in view of adding bidirectionality to a rasorber, it is necessary to investigate the variation in the resonance with respect to impedance at the two resonance frequencies (low and high). One of the ways to do this is to model the equivalent circuit of the dual-sided metasurface structure individually at the low and high resonance frequencies.

The equivalent circuit model (ECM) of the dual-sided metasurface structure has been designed based on the unidirectional metasurface structures working in the microwave and THz regime [85-86]. For the analysis purpose, the coupling between the adjacent unit cells of the metasurface structure has been ignored. The mutual coupling between the adjacent unit cells depends on the distance of separation between them. If the separation is large, the mutual effect between adjacent unit cells is minimal [87]. The result shown in [88] suggests that ignoring mutual effect between adjacent unit cells does not show any variation in the simulated and circuit modelling responses.

The ECM of the dual-sided metasurface structure is shown in Fig. 4.7(a). The ECM consists of a series combination of $R_1 - L_1 - C_1$ (corresponding to the metallic pattern of metasurface 1) connected in parallel to the series combination of $R_2 - L_2 - C_2$ (corresponding to the metallic pattern of metasurface 2). In between metasurface 1 and metasurface 2, the dielectric layer is

modelled as a transmission line of length h and characteristics impedance Z_{diel}, where $Z_{diel} = \frac{Z_o}{\sqrt{\varepsilon_r}}$ [89]. Z_o is the characteristics impedance of free space. For all the calculations, $+z$ incident electromagnetic (EM) wave has been considered. However, the analysis is equally valid for -*z* incident EM wave too.

From the ECM, it can be observed that the total impedance of the dual-sided metasurface structure seen by the incident EM wave can be expressed as equation. (4.1).

$$Z_{total} = (R_1 + j(\omega L_1 - \frac{1}{\omega C_1})) \,||\, Z_{in1} \tag{4.1}$$

The transformation of impedance Z_{meta2} to Z_{in1} can be calculated by equation. (4.2) [90].

$$Z_{in1} = Z_{diel} \frac{Z_{meta2} + jZ_{diel} \tan(\beta_1 h_1)}{Z_{diel} + jZ_{meta2} \tan(\beta_1 h_1)} \tag{4.2}$$

Here, $\beta_1 h_1$ is the electrical length of the transmission line and Z_{meta2} is the impedance of metasurface 2, expressed as, $Z_{meta2} = (R_2 + j(\omega L_2 - \frac{1}{\omega C_2}))$

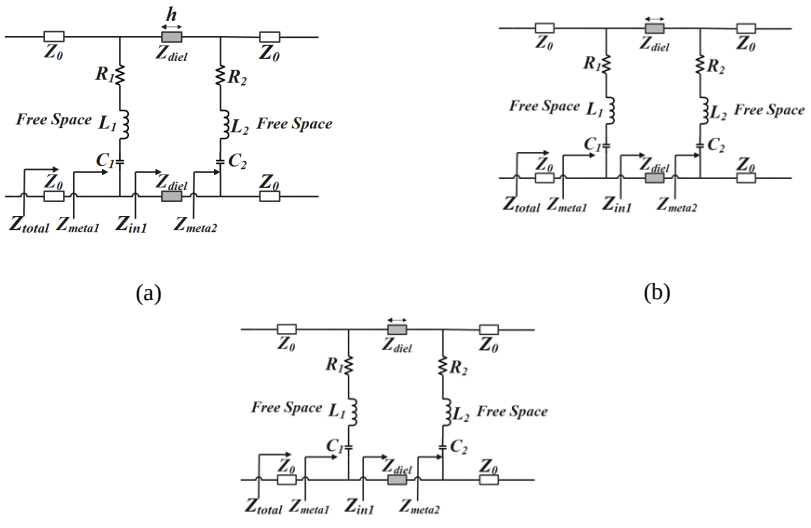

Fig. 4.7. (a) Equivalent circuit model of the dual-sided metasurface structure, Equivalent circuit modelling at (b) low and (c) high frequencies.

4.4.1. EQUIVALENT CIRCUIT MODEL OF THE STRUCTURE AT HIGH RESONANCE FREQUENCY

The ECM of the dual-sided metasurface structure at low resonance frequency is shown in Fig. 4.7(b). At low resonance frequency, the size of the dielectric is very small as compared to the resonating wavelength $\sim \frac{\lambda}{70}$. Under this condition, the electrical length $\beta_1 h_1$ of the transmission line become so small that the imaginary term in equation. (4.2) can be ignored. Equivalently, the presence of transmission line in between metasurface 1 and metasurface 2 can be ignored, as apparent from Fig. 4.7(b). The total impedance Z_{total} seen by incident EM wave will be equal to $Z_{meta1} \,||\, Z_{meta2}$.

$$Z_{total} = \frac{(R_1 + j(\omega L_1 - \frac{1}{\omega C_1}))(R_2 + j(\omega L_2 - \frac{1}{\omega C_2}))}{(R_1 + j(\omega L_1 - \frac{1}{\omega C_1})) + (R_2 + j(\omega L_2 - \frac{1}{\omega C_2}))} \tag{4.3}$$

Considering the values of the respective impedances, the total impedance of the dual-sided metasurface structure seen by the incident EM wave is derived in equation. (4.3). From the expression of Z_{total}, it can be observed that the expression remains unaltered regardless of the direction of the incident wave. The identical impedance value for either side incidence leads to the identical resonance point in the structure.

4.4.2 Equivalent circuit model of the structure at high resonance frequency

The ECM of the dual-sided metasurface structure at high resonance frequency is shown in Fig. 4.7(c). At high resonant frequency, the ratio between resonating wavelength and structure thickness is large, and hence the presence of the transmission line between metasurface 1 and metasurface 2 cannot be ignored. The presence of transmission line affects the transformation of impedances in such a way that $Z_{in1} \neq Z_{meta2}$. Under such conditions, the total impedance seen

by the wave when incident from +z and –z direction has been derived in equation (4.4) and equation. (4.5) respectively.

$$Z_{total(+z)} = \frac{Z_{diel}X_1X_2 + jZ_{diel}^2X_1\tan(\beta_1h_1)}{Z_{diel}(X_1+X_2) + jX_1X_2\tan(\beta_1h_1) + jZ_{diel}^2\tan(\beta_1h_1)} \quad (4.4)$$

$$Z_{total(+z)} = \frac{Z_{diel}X_1X_2 + jZ_{diel}^2X_2\tan(\beta_1h_1)}{Z_{diel}(X_1+X_2) + jX_1X_2\tan(\beta_1h_1) + jZ_{diel}^2\tan(\beta_1h_1)} \quad (4.5)$$

Here, X_1 is the notations used for the impedance of metasurface 1 (Z_{meta1}) and X_2 is the notation used for the impedance of metasurface 2 (Z_{meta2}). With the proper analyses of the expression of net impedances in equations. 4.4 and 4.5, it is evident that the total impedance seen by the EM wave for +z and -z incidence depends on the individual impedances of metasurface 1 and metasurface 2 i.e., X_1 and X_2. As the metallic patterns of metasurface 1 and metasurface 2 are different, their impedance values (X_1 and X_2) will also be different, leading to the change in the frequency of resonance for change in the direction of incidence.

4.5. Realization of a bidirectional rasorber

Finally, to validate the study done in sections 4.3 and 4.4, a bidirectional rasorber is designed in this section. It is already discussed that any dual-sided metasurface structure always resonates at two different frequencies where at the low resonance frequency, the structure works like a bandpass filter having a high transmission value whereas at high resonance frequency, the structure behaves like an absorber with a low transmission value. A bidirectional rasorber means that the device should exhibit identical frequency response for +z as well as -z incidences. However, from equations. (4.4) and (4.5) it is apparent that the variation in the response of the dual-sided metasurface structure for +z and -z incidence is due to the variation in the impedance values of metasurface 1 and metasurface 2. Therefore, to get a uniform response for either direction of incidence, the optimization of the metallic patterns of

metasurface 1 and metasurface 2 should be such that the impedance of the metallic pattern at metasurface 1 and metasurface 2 should be equal viz., $X_1 = X_2$.

The setup of the bidirectional rasorber for +*z* and -*z* incidences along with the electromagnetic field vectors are shown in Fig. 4.8(a) and Fig. 4.8(b) respectively. The optimized metallic pattern at the top and bottom metasurface layers are shown in Fig. 4.8(c) and Fig. 4.8(d) respectively. For the metallic components, gold has been taken and for the dielectric ZnSe has been considered. The thickness of the dielectric layer is optimized as 0.22 μm, while the thickness of the metallic component of gold has been taken as 0.06 μm. The optimized geometrical dimensions of the rasorber have been mentioned in Fig. 4.8.

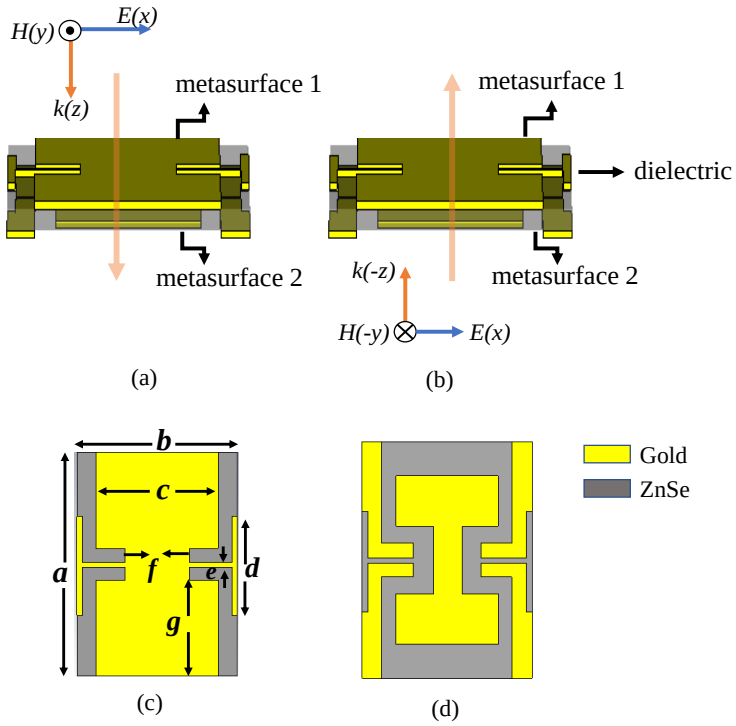

Fig. 4.8. 3-D perspective view of the unit-cell of the bidirectional rasorber for (a) +z incidence (b) -z incidence and (c) metallic pattern on metasurface 1 and (d) metallic pattern on metasurface 2 (a = 3.95 μm, b = 3.29 μm, c = 2.5 μm, d = 2.04 μm, e = 0.11 μm, f = 1.31 μm, g = 2.1 μm).

The curve of the reflection and transmission coefficients of the bidirectional rasorber for +z and -z incidences have been shown in Fig. 4.9(a) and Fig. 4.9(b) respectively. It can be seen

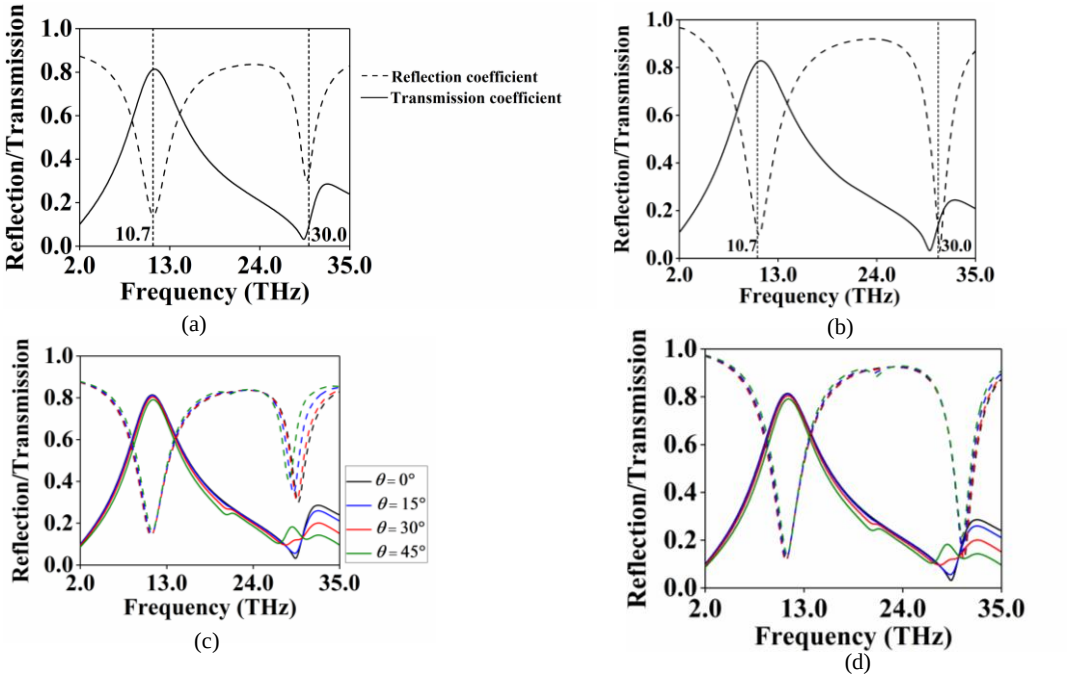

Fig. 4.9. Reflection and transmission coefficient response of the rasorber for (a) +z and (b) -z incidence and oblique incidence response of the structure under TE polarization for (c) +z and (d) -z incidence.

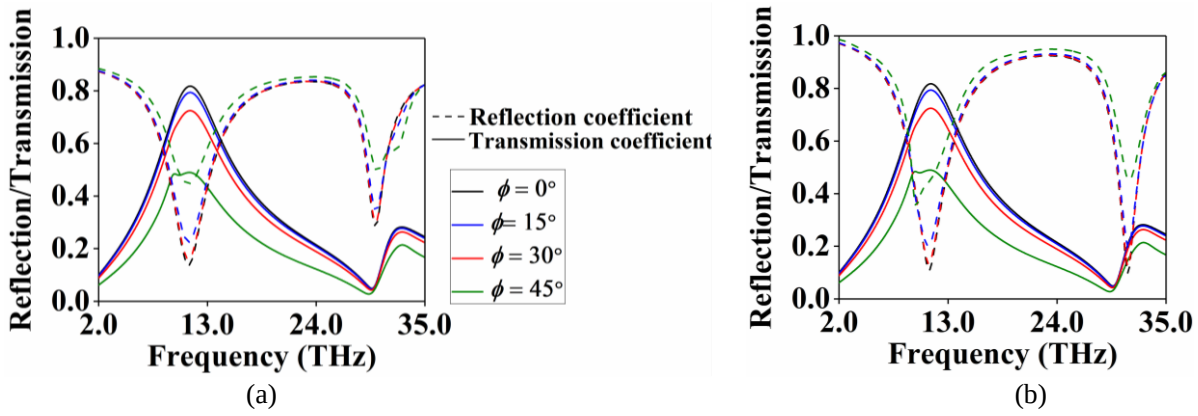

Fig. 4.10. Reflection and transmission coefficient response of the rasorber for different polarization angles under normal incidence of the proposed structure for (a) +z and (b) -z incidence.

from the response that the rasorber exhibits an identical frequency response for either side

incidence. The structure behaves like a band pass filter at 10.7 THz and absorber at 30.0 THz for +z as well as -z incidences. Additionally, the structure is studied for different angles of incidences under TE polarization and it has been found that up to 45^o, the structure is behaving as a bidirectional rasorber, as evident from Fig. 4.9(c) and Fig. 4.9(d). The structure is further studied under polarization angle variation for normal incidence as shown in Fig. 4.10, where it has been found that for both side incidences the structure behaves as a bidirectional rasorber till 30^o polarization angle.

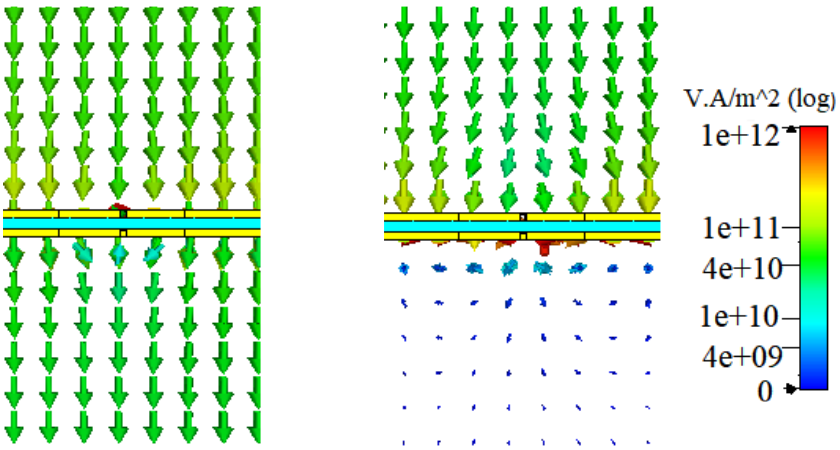

(a) (b)

Fig. 4.11. Power flow from the rasorber at (a) low frequency (10.7 THz) and (b) high frequency (30 THz).

Fig. 4.11 depicts the power flow from the structure at the low and high resonance frequencies. It is evident from Fig. 4.11(a), that at the low resonance frequency (10.7 THz), the structure offers a complete transmission, signifying the bandpass characteristics of the rasorber. In contrast, Fig. 4.11(b) illustrates that there is negligible amount of power flow from the structure at high resonance frequency (30.0 THz), signifying absorption in the structure.

4.7. Conclusions

Driven by the advancement in the wireless technology and size miniaturization, it is desirable to design devices which offers multifunctionality as well as bidirectionality to the electronic

sub-system. A dual-sided metasurface structure consisting of two different sets of metasurface on its two sides offers a promising future for the design of such devices. However, the selection of metasurface pattern in a dual-sided metasurface structures is extremely challenging as compared to their unidirectional counterpart.

The work presented in this chapter has investigated the characteristics behaviour of a dual-sided metasurface structure. It has been demonstrated that the relation between wavelength of the resonance and the thickness of the structure plays a key role in switching the mode of operation from transmission to absorption and vice-versa. Also, we have investigated the equivalent circuit model of the dual-sided metasurface design to mathematically analyze the role of impedance in achieving bidirectionality in multifunctional devices. In view of validating the proposed concept of multifunctionality and bidirectionality a bidirectional rasorber is consequently designed.

CONTENTS

Chapter 5: A metasurface based broadband cross polarization converter for far infrared region